Front. Optoelectron. China 2010, 3(1): 22–32
DOI 10.1007/s12200-009-0079-8

RESEARCH ARTICLE

# Physical mechanism of "slow light" in stimulated Brillouin scattering

**Valeri I. KOVALEV (✉)[1,2], Robert G. HARRISON[1], Nadezhda E. KOTOVA[1,2]**

1 Department of Physics, Heriot-Watt University, Edinburgh EH14 4AS, UK
2 P. N. Lebedev Physical Institute, Russian Academy of Sciences, Moscow 119991, Russia

© Higher Education Press and Springer-Verlag Berlin Heidelberg 2010

**Abstract** We show from analytical analysis of the basic stimulated Brillouin scattering (SBS) equations in the time domain that the SBS amplification process does not amplify an external Stokes pulse and therefore cannot induce group delay of the Stokes pulse as claimed in the literature. Rather, the delayed output Stokes pulse is the pump radiation reflected by the induced acoustic wave, the amplitude of which determines the rate of the amplification process and time delay of the pulse. The latter is predominantly a consequence of the SBS buildup process determined by the inertia of the acoustic wave excitation. Analytical solutions of the SBS equations in the frequency domain show that spectral broadening of the pump radiation leads to only negligible broadening of the SBS spectral bandwidth and so does not provide an effective means to achieve broadband pulse delay.

**Keywords** stimulated Brillouin scattering (SBS), pulse delay, acoustic wave inertia, spectral bandwidth

## 1 Introduction

It is well known that the group velocity of a light pulse in a medium is smaller than the phase velocity, $c/n$, of monochromatic light, where $c$ is the speed of light in vacuum and $n$ is the refractive index of a medium [1]. This is because a pulse is generically composed of a range of frequencies, and the refractive index, $n$, of a material is not constant but depends on the frequency, $\omega$, of the radiation, $n = n(\omega)$. A group index $n_g(\omega) = n + \omega(\mathrm{d}n/\mathrm{d}\omega)$ is used to quantify the delay (or advancement), $\Delta t_g$, of an optical pulse, $\Delta t_g = n_g L/c$, which propagates in a medium of length $L$, where $c/n_g$ is called the group velocity. Such pulse group delay is now commonly termed "slowing down" of light [2].

In general, group delay is very small for propagation of light pulses through optically transparent media. However, when the light resonantly interacts with the medium, group delay may be greatly enhanced. Widely ranging applications for such slow light (SL) have been proposed, of which those for telecommunication systems and devices (optical delay lines, optical buffers, optical equalizers, and signal processors) are currently of most interest. The essential demand of such devices is compatibility with existing telecommunication systems, that is, they must be of wide enough bandwidth ($\geqslant 10$ GHz) and able to be integrated seamlessly into such systems [3].

Of the various nonlinear resonance mechanisms and media considered, stimulated Brillouin scattering (SBS) in optical fiber is deemed to be among the best candidates [4]. Along with obvious device compatibility, there are several other advantages of the SL via SBS for optical communications systems: slow-light resonance can be created at any wavelength by changing the pump wavelength; use of optical fiber allows for long interaction lengths and thus low powers for the pump radiation, the process runs at room temperature, it uses off the shelf telecom equipment, and SBS works in the entire transparency range of fibers and in all types of fiber.

In the SBS interaction, the pulse to be delayed is a frequency downshifted (Stokes) pulse. This is transmitted through an optical fiber through which continuous wave (CW) pump radiation is sent in the opposite direction to prime the delay process. It is supposed that the Stokes pulse is amplified by parametric coupling with the pump wave and a material (acoustic) wave in the medium [5], and the amplification is characterized by a resonant-type gain profile. The dispersion of refractive index associated with this profile can then, it is claimed, be used to increase the group index for optical pulses at the Stokes frequency [6]. These features are illustrated in Fig. 1, which shows

Received August 1, 2009; accepted August 28, 2009

E-mail: v.kovalev@hw.ac.uk

the gain spectral profile together with its refractive index dispersion profile [7], the gradient of which results in $n_g(\omega)$.

Many experimental results on pulse delaying via SBS in optical fiber have been published in the last few years (see the review paper [4] and references therein). However, interpretation of these results based on group index-induced delay as discussed above appears to be in contradiction with the basics of the SBS phenomenon.

In this paper, we address this and examine the physical reasons why an output Stokes pulse is delayed through SBS. We show from analytical analysis of the basic SBS equations in the time domain that the amplification process does not amplify an external Stokes pulse and therefore cannot induce group delay of the Stokes pulse as is claimed in the literature. Rather, the delayed output Stokes pulse is, as we show, predominantly a consequence of SBS buildup, which is determined by inertia of the acoustic wave excitation. It is further claimed in the literature that spectral broadening of the pump radiation gives rise to similar broadening of the SBS spectral gain bandwidth, thereby providing a way to achieve broadband operation. However, we show through analysis of the SBS equations in the frequency domain that pump radiation broadening by any reasonable amount has only a negligible effect on increasing the SBS bandwidth.

## 2 Basic SBS equations

In SBS, the resonance in a medium's response occurs at and around the Brillouin frequency, $\Omega_B$, which is the central frequency of the variation of density in a medium,

$$\delta\rho(z,t) = \frac{1}{2}[\rho(z,t)\mathrm{e}^{-\mathrm{i}(\Omega_B t+qz)} + \mathrm{c.c.}].$$

This density variation is resonantly enhanced by an electrostrictive force resulting from interference of two plane counter-propagating waves, the forward-going ($+z$ direction) Stokes and backward-going ($-z$ direction) pump optical fields,

$$\mathrm{E_S}(z,t) = \frac{1}{2}[E_S(z,t)\mathrm{e}^{-\mathrm{i}(\omega_S t-k_S z)} + \mathrm{c.c.}]$$

and

$$\mathrm{E_p}(z,t) = \frac{1}{2}[E_p(z,t)\mathrm{e}^{-\mathrm{i}(\omega_p t+k_p z)} + \mathrm{c.c.}],$$

respectively, where $\rho(z,t)$, $E_S(z,t)$, and $E_p(z,t)$ are the amplitudes of the acoustic wave and of Stokes and pump fields, with $\Omega = \omega_p - \omega_S$ and $q = k_p + k_S$, $\omega_S$ and $k_S$, and $\omega_p$ and $k_p$ being their radian frequencies and wave vectors, and c.c. is the abbreviation for complex conjugate. In an isotropic medium, $\delta\rho(z,t)$ is described by the following equation [8]:

$$\frac{\partial^2\delta\rho}{\partial t^2} - v_s^2\nabla^2\delta\rho - A\nabla^2\frac{\partial\delta\rho}{\partial t} = -\rho_0\frac{\partial\varepsilon}{\partial\rho}\frac{1}{16\pi}\nabla^2|\mathrm{E}(z,t)|^2, \quad (1)$$

where $v_s$ is the velocity of a free acoustic wave, $A$ is its damping parameter, $\nabla^2 \equiv \partial^2/\partial z^2$ in the chosen plane wave model, $\varepsilon$ and $\rho_0$ are the dielectric function and equilibrium density of the medium, and $\mathrm{E}(z,t) = \mathrm{E_p}(z,t) + \mathrm{E_S}(z,t)$. Since the amplitude $\rho(z,t)$ is supposed to be slowly varying in space, then

$$\nabla^2\delta\rho(z,t) \approx -q^2\delta\rho(z,t),$$

and Eq. (1) is usually reduced to

$$\frac{\partial^2\delta\rho}{\partial t^2} + \Omega_B^2\delta\rho + \frac{\Gamma_B}{2}\frac{\partial\delta\rho}{\partial t} = -\rho_0\frac{\partial\varepsilon}{\partial\rho}\frac{1}{8\pi}\frac{\partial^2}{\partial z^2}[\mathrm{E_p}(z,t)\mathrm{E_S^*}(z,t)]. \quad (2)$$

This is then the equation for the induced acoustic wave. It is a typical equation for an externally driven damped resonant oscillator, in which the right-hand side (RHS) is the driving force,

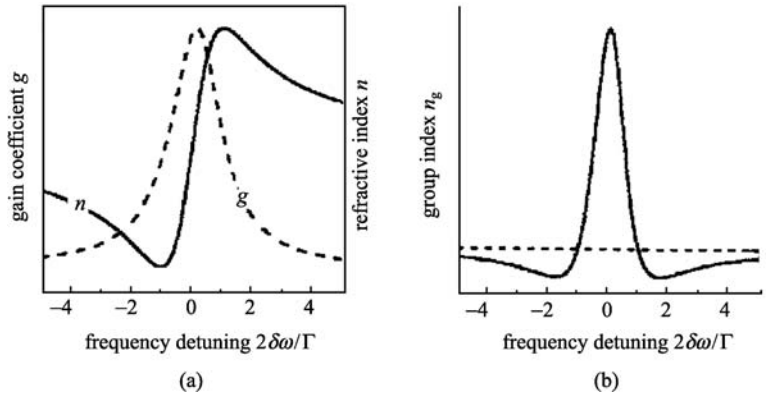


**Fig. 1** Normalized dispersion of gain coefficient, $g(\omega)$ (dashed line), refractive index, $n(\omega)$, and group index, $n_g(\omega)$ of SBS

$$\Omega_B = qv_s = \frac{2nv_s\omega_p}{(c/n)+v} \approx \frac{2nv_s\omega_p}{c}$$

is the resonant frequency of the oscillator, known as the Brillouin frequency, and $\Gamma_B$ is the full width at half maximum (FWHM) spectral width of the resonant profile, with $2/\Gamma_B$ being the decay time of the acoustic wave.

The pump field reflected by the induced acoustic wave is a new Stokes field, which in turn interacts with the pump field to further electrostrictively enhance the acoustic wave and so the Stokes field and so forth. Increase of the Stokes field in SBS is therefore a direct consequence of the increase of reflectivity of the acoustic wave for the pump field. As such, so-called "SBS gain" characteristics are determined by the reflectivity, spectral characteristics, and dynamics of the acoustic wave. In the approximation that the CW pump radiation is not depleted over the interaction length, $L$, the spatial/temporal evolution of the Stokes signal is described by the nonlinear wave equation,

$$\frac{\partial^2 E_S}{\partial z^2} - \frac{\varepsilon}{c^2}\frac{\partial^2 E_S}{\partial t^2} = \frac{1}{c^2}\frac{\partial \varepsilon}{\partial \rho}\frac{\partial^2}{\partial t^2}[\delta\rho(z,t)E_p(z,t)]. \quad (3)$$

Equations (2) and (3) are the basic equations, which describe the SBS phenomenon in an optically lossless medium in the small signal plane wave approximation. Since the density and Stokes field amplitudes, $\rho(z,t)$ and $E_S(z,t)$, vary slowly in both space and time and the acoustic wave in SBS attenuates strongly, their evolution is usually reduced to two well-known first-order equations: from Eq. (2), the relaxation equation for $\rho(z,t)$:

$$\frac{\partial \rho}{\partial t} + \left(\frac{\Gamma_B}{2} + i\delta\Omega\right)\rho = -i\rho_0\frac{\partial \varepsilon}{\partial \rho}\frac{\Omega_B}{8\pi v_s^2}E_p(t)E_S^*(z,t), \quad (4)$$

which describes the amplitude of the driven damped resonant oscillator, and from Eq. (3), the partial differential equation for $E_S(z,t)$,

$$\frac{\partial E_S}{\partial z} + \frac{n}{c}\frac{\partial E_S}{\partial t} = -i\frac{\omega_S}{2cn}\frac{\partial \varepsilon}{\partial \rho}\rho^*(z,t)E_p(t). \quad (5)$$

Here, $\delta\Omega = \Omega - \Omega_B$ is the difference between the acoustic drive frequency, $\Omega$, and the resonant Brillouin frequency, and asterisk, *, marks complex conjugate. The RHS of Eq. (5) is a source of the Stokes emission.

## 3 Effect of acoustic wave inertia on Stokes pulse delay in SBS

In this section, we address the physical mechanism that gives rise to delay of a Stokes pulse in the presence of SBS. In typical SBS-based SL experiments, the CW pump power is kept below the value at which the SBS interaction experiences pump depletion. The pump power is therefore constant throughout the interaction length (in lossless media). This is also an underlying reason why the contribution of spontaneous scattering to the SBS interaction is considered sufficiently small to be ignored in theoretical treatments of this problem [7,9,10]. Equations (4) and (5) with appropriate boundary conditions are therefore sufficient for describing the evolution of a Stokes pulse in a medium.

It is convenient to introduce the new temporal coordinate $t' = t - zn/c$ and suppose that the center frequency of the Stokes pulse spectrum coincides with the resonant Brillouin Stokes frequency, that is, $\delta\Omega = 0$. In terms of the new variables, Eqs. (4) and (5) can be rewritten as

$$\frac{\partial \rho}{\partial t'} + \frac{1}{\tau}\rho = -i\rho_0\frac{\partial \varepsilon}{\partial \rho}\frac{\Omega_B}{8\pi v_s^2}E_pE_S^*(t') \quad (6)$$

and

$$-\frac{\partial E_S}{\partial z} = -i\frac{\omega_S}{2cn}\frac{\partial \varepsilon}{\partial \rho}\rho^*(t')E_p. \quad (7)$$

This set of equations has an analytical solution, which can be obtained using Riemann's method [11]. Consider the case addressed in typical SL experiments, in which the duration of the Stokes pulse is much less than its transit time in the medium and the pump is CW monochromatic radiation. Assuming that there are no acoustic waves in the medium before a Stokes pulse enters, and $E_S(t' \leqslant 0) = 0$, $E_S(z = 0,t') = E_{S0}(t')$, and $E_p(z,t') \equiv E_p = \text{const}$, the solutions for the Stokes field and the density variation are then

$$E_S(z,t') = E_{S0}(t') + \frac{gI_pz}{\tau}\int_0^{t'}\left(e^{-\frac{t'-\vartheta}{\tau}}\right) \cdot I_1\left(\sqrt{2gI_pz\frac{t'-\vartheta}{\tau}}\right)\sqrt{2gI_pz\frac{t'-\vartheta}{\tau}}E_{S0}(\vartheta)d\vartheta \quad (8)$$

and

$$\rho(t') = -i\rho_0\frac{\partial \varepsilon}{\partial \rho}\frac{\Omega_B}{8\pi\tau v_s^2}E_p\int_0^{t'}\left(e^{-\frac{t'-\vartheta}{\tau}}\right) \cdot I_0\left(\sqrt{2gI_pz\frac{t'-\vartheta}{\tau}}\right)E_{S0}^*(\vartheta)d\vartheta. \quad (9)$$

Here, $I_p = |E_p|^2$ is the pump radiation intensity in W/cm$^2$, $I_0(x)$ and $I_1(x)$ are the Bessel functions of the imaginary argument $x$, and $g$ is the SBS gain coefficient,

$$g = 10^7\frac{\omega_S^2\rho_0\tau}{4nc^3v_s}\left(\frac{\partial \varepsilon}{\partial \rho}\right)^2 \quad (\text{cm/W}). \quad (10)$$

Equation (8) explicitly shows that the input Stokes pulse (the first term on the RHS) is transmitted through the medium unmodified. The second term is the result of reflection of the pump field by the acoustic wave. As such,

it retains the features of buildup of the acoustic wave and its dynamics as described by Eq. (9).

Suppose that the input Stokes signal is an optical pulse, the time-dependent intensity of which is given by

$$I_S(z=0,t) = |E_S(z=0,t)|^2$$

$$= I_{S0}(3.5t/t_p)^2 e^{-3.5t/t_p}, \qquad (11)$$

where $I_{S0}$ is the intensity at the peak of the pulse and $t_p$ is the FWHM pulse duration. The shape of the pulse is shown in Figs. 2 and 3 (curves for $G = gI_pL = 0$) and it is a good approximation for pulses actually used in laser experiments [12]. Since the SBS exponential gain, $G$, in the fiber is supposed to be below the SBS threshold, this, according to our recent work [13], limits $G$ to $\leqslant 12$ for standard silica fibers of $> 0.1$ km length.

Figures 2 and 3 show the calculated relative output Stokes pulse powers, $P_S(t) = |E_S(t)|^2 S$ ($S$ is the effective area of fiber-mode cross-section), shapes, amplitudes, and delays for four input pulse durations, $t_p$, and different $G$. Here, the decay time, $\tau$, of the hyper-sound wave in silica is taken to be $\tau = 18$ ns at a pump radiation wavelength ~1.55 μm. It should be emphasized that the decay time of the acoustic wave, which is determined by the viscosity of fused silica [14], is used in these calculations rather than the SBS spectral width. This is because the latter depends on intrinsic characteristics of the fiber (core/cladding design, doping type and concentration, numerical aperture, etc. [15–17]) and the ambient environment (mechanical, thermal, and electromagnetic fields [15]), all of which can result in substantial variation of the resonant Brillouin frequency, $\Omega_B$. However, they do not appreciably affect the viscosity of the medium.

It follows from Figs. 2 and 3 that the induced delay, $\Delta T_d$, of the output Stokes pulse and its duration in all cases increase with increase of $G$. Rates of these growths depend substantially on the ratio of pulse duration to acoustic wave decay time, $t_p/\tau$, as shown in Fig. 4.

For a long input Stokes pulse, $t_p = 200$ ns, that is, $t_p/\tau = 200/18 \gg 1$, the output pulse, on increase of $G$, remains similar in form (Fig. 2(a)) and is increasingly delayed following $\Delta T_d/G \approx 11$ ns as shown by the thick dashed line in Fig. 4(a).

Additional calculations have shown that it may coincide with $\Delta T_d \approx \tau G/2 \approx 9G$ ns (shown by the thin solid line in Fig. 4(a)), but this happens only when $t_p/\tau \approx 2.5 \pm 0.5$ and $> 100$. For $t_p/\tau < 2$, the growth of $\Delta T_d$ falls below the value $\Delta T_d \approx 9G$ ns. The duration of the output pulse compared to that of the input is slightly broadened with increase of $G$ (see dashed line in Fig. 4(b)).

For $t_p = 18$ ns (Fig. 2(b)), that is, $t_p/\tau = 1$, $\Delta T_d$ for the output pulse again increases with $G$, although not linearly; at lower $G$ (0 to ~2) with slope $\Delta T_d/G \approx 3$ ns and at higher $G$ ($> 2$) with slope $\Delta T_d/G \approx 9$ ns (dotted line in Fig. 4(a)). The pulse broadening in this case increases substantially with $G$, by a factor $\geqslant 5$ at $G > 10$ (dotted line in Fig. 4(b)).

For the short pulses, $t_p \leqslant 4$ ns (Fig. 3), that is, for $t_p/\tau < 1$, significant new features appear. For $G < 4$, the output pulses approximately retain their shape with only a slight increase of $\Delta T_d$ with $G$ ($\Delta T_d/G \approx 0.1 - 0.15$ ns for $t_p = 4$ ns and $\Delta T_d/G \approx 0.03$ ns for $t_p = 0.5$ ns, as shown in the inset of Fig. 4(a), solid and dashed lines, respectively). For $G$ between 4 and 6, there is substantial growth of the power in the tail of the pulses, and for $G > 8$, the maximum of the pulse shifts to the tail (as shown in Figs. 3(a) and 3(b)). This is because of the long decay of the acoustic wave excited by the short Stokes pulse interacting with the CW pump. The dependence of $\Delta T_d$ on $G$ for $G > 8$ then follows the linear relation $\Delta T_d \approx 9G - 25$ ns (thick solid line in Fig. 4(a)). The pulse broadening factor is then ~20 for $t_p = 4$ ns (solid line in Fig. 4(b) at $G > 6$) and ~200 for $t_p = 0.5$ ns.

It is interesting to note that our analytical results presented in Figs. 2–4, which are obtained in the small signal limit, give dependencies of pulse delay and broadening on $G$ quite similar to those obtained numerically both for long pulses, $t_p/\tau \approx 15$ and 5 in Ref. [10], and for short pulses, $0.1 < t_p/\tau < 2$ in Ref. [18]. There are,

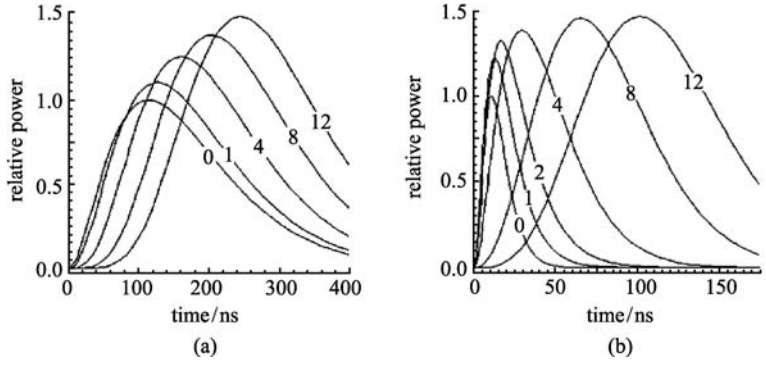


**Fig. 2** Output Stokes pulse shapes. (a) $t_p = 200$ ns ($\gg \tau$) and $G = 0$ (1), 1 (0.42), 4 (0.026), 8 (0.0006), and 12 (0.000012); (b) $t_p = 18$ ns ($= \tau$) and $G = 0$ (1), 1 (0.9), 2 (0.6), 4 (0.2), 8 (0.09), and 12 (0.00026) (numbers in parentheses are the amplitude magnification factors; numbers on curves are $G$)

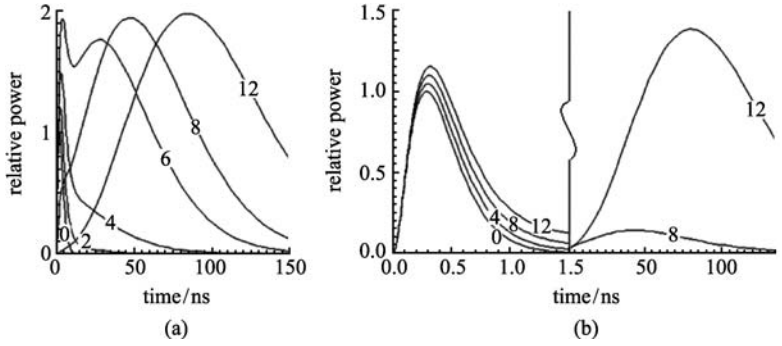


**Fig. 3** Output Stokes pulse shapes. (a) $t_p = 4$ ns ($< \tau$) and $G = 0$ (1), 2 (1), 4 (1), 6 (1), 8 (0.2), and 12 (0.007); (b) $t_p = 0.5$ ns ($\ll \tau$) and $G = 0$ (1), 4 (1), 8 (1), and 12 (1 at the first peak and 0.3 at the tail) (Left-hand side (LHS) of (b) is temporally stretched to show profiles)

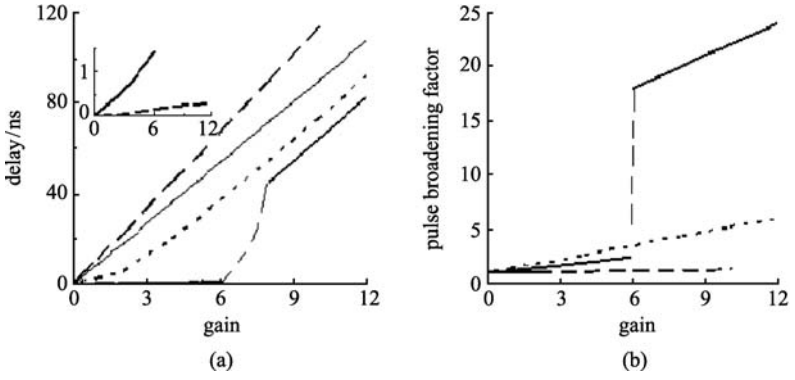


**Fig. 4** Output Stokes pulse. (a) Delay and (b) broadening factor versus gain $G$ for pulse durations $t_p = 200$ (dashed), 18 (dotted), 4 (thick solid in the main graph and in the inset), and 0.5 ns (dashed in the inset) (Thin solid line in (a) is $\Delta T_d = 9G$ ns dependence)

however, some quantitative differences that, we think, are important to highlight. The numerical modeling in Ref. [10] gives $\Delta T_d = \tau G/2$ dependence for $t_p/\tau \approx 15$, while our calculations predict this only for $t_p/\tau$ in the region $\sim 2.5 \pm 0.5$; for $t_p/\tau > 5$, the slope $\Delta T_d/G$ is a factor 1.2–1.3 steeper. Also, the shape of the $\Delta T_d$ upon $G$ dependence for $t_p/\tau \approx 5$ in Ref. [10] is similar to that in our calculations but for $t_p/\tau \approx 1$. As to the numerical results presented in Ref. [18], the difference with our findings is most probably because all their results were obtained for an input Stokes power well above that for onset of pump depletion (input Stokes power is of 1 mW compared with pump power of $\leqslant 20$ mW).

## 4 Dynamics and spectrum of acoustic wave amplitude

To understand the nature of the behavior described above, consider through Eq. (9) the temporal and spectral characteristics of the complex dielectric function variation in the medium, $\Delta\varepsilon = (\partial\varepsilon/\partial\rho)\rho = \Delta\varepsilon' + i\Delta\varepsilon''$, induced by the interaction of the pump and Stokes signals; $\Delta\varepsilon''(\omega)$ is usually attributed to SBS gain and $\Delta\varepsilon'(\omega)$ to modification of the refractive index, $\Delta n(\omega) \approx \Delta\varepsilon'(\omega)/(2n_0)$, of the medium, where $n_0$ is the refractive index of a medium without SBS. In the limit of small gain, $G < 1$, the Bessel function $I_0(x)$ in Eq. (9) may be set to unity, and analysis is greatly simplified. While this approximation does not allow us to describe gain narrowing of the SBS spectrum typical for higher $G$, it still captures reasonably well the trends in the temporal and spectral features of $\rho$, which determine those of the SBS gain and modified refractive index.

When $I_0(x) = 1$, the integral in Eq. (9) can be taken for $E_{S0}(t)$ given by Eq. (11). It results in the following analytical expression for $\rho(t)$:

$$\rho(t) = A\left\{\frac{2}{(2b-\tau)^2}\left[2\tau b\left(e^{-\frac{t}{\tau}} - e^{-\frac{t}{2b}}\right) + (2b-\tau)te^{-\frac{t}{2b}}\right]\right\}, \tag{12}$$

where $b = t_p/3.5$ and $A = -i\rho_0\frac{\partial\varepsilon}{\partial\rho}\frac{\Omega_B}{8\pi v^2}E_p E_S^*(0)$. The spectral characteristics of the acoustic wave amplitude follow from the Fourier transform of Eq. (12):

$$\rho(\omega) = A\sqrt{\frac{2}{\pi}}\frac{4\tau b}{(2b-\tau)^2}\left[\tau\frac{1+i\tau\omega}{1+(\tau\omega)^2} - 2b\frac{1+i2b\omega}{1+(2b\omega)^2}\right]$$

$$+\sqrt{\frac{2}{\pi}}\frac{8b^2}{(2b-\tau)}\frac{1+\mathrm{i}4b\omega-(2b\omega)^2}{[1+(2b\omega)^2]^2}. \qquad (13)$$

The temporal dynamics of the induced acoustic wave amplitudes and their spectra for values of $t_p/\tau$ considered above are shown in Fig. 5 (the dynamics for $t_p = 0.5$ ns is not shown on the timescale of Fig. 5(a)). The curves in Fig. 5(a) represent different characteristic types of SBS interaction: curves 1 give an example of quasi-steady-state interaction when $t_p/\tau \gg 1$, curves 3 demonstrate transient-type interaction when $t_p/\tau \ll 1$, and curves 2 are for an intermediate case when $t_p/\tau \approx 1$.

In the first case of a long Stokes pulse, that is, $t_p/\tau \gg 1$, the shape of the acoustic wave pulse shown in Fig. 5(a) as the solid curve 1 almost reproduces the shape of the input Stokes pulse (dotted curve 1). The spectrum of the excited acoustic wave in this case (Fig. 5(b)) reproduces the spectrum of the input Stokes pulse, as shown by the solid and dashed curves 1, respectively. These are both narrower than the Lorentzian-shaped spectrum corresponding to $\tau =$ 18 ns (dotted curve 5).

This is to be expected since Eq. (2) is, in essence, the equation for the amplitude of a driven damped oscillator; for such a system, the spectrum of the induced oscillations is fully determined by the spectrum of the driving force when it is narrower than reciprocal decay time of the oscillator.

In the case of shorter Stokes pulses, $t_p/\tau \leqslant 1$ (dashed curves 2 and 3 in Fig. 5(a)), the spectrum of the driving force, that is, that of the input Stokes pulse, is broadband (dashed curves 2 and 3 and also curve 4 for $t_p = 0.5$ ns pulse in Fig. 5(b)). As seen, the dynamics of the medium's response (solid curves 2 and 3 in Fig. 5(a)) and its spectra (solid curves 2, 3, and 4 in Fig. 5(b)) differ substantially from those of the Stokes pulses and their spectra. In the temporal domain, the maximum amplitude of the induced $\rho(t)$ decreases with decrease of pulse duration and a long tail appears after a Stokes pulse, which decays exponentially with a decay time $\tau$. The spectra of $\rho(t)$ in these cases are narrower, increasingly so for shorter pulses, than the spectra of the driving force (input Stokes pulse). Their width is then determined predominantly by the reciprocal decay time of the oscillator (dotted curve 5 in Fig. 5(b)) as is to be expected for a damped oscillator, which is driven by a broadband force.

The imaginary part of $\rho(\omega)$ described by Eq. (13) gives the refractive index of the medium modified by the SBS interaction,

$$n(\omega) = n_0 + \Delta n(\omega) \approx n_0 + \frac{(\partial\varepsilon/\partial\rho)\rho(\omega)}{2n_0},$$

and its corresponding group index,

$$n_g(\omega) = n_0 + \omega\frac{\mathrm{d}\Delta n(\omega)}{\mathrm{d}\omega}.$$

Spectra of the Stokes pulses and the group indices induced by these pulses are shown in Fig. 6 for the four different $t_p/\tau$.

It is clear from Fig. 6 that the spectral width of a Stokes pulse is wider than that of the SBS-induced group index regardless of $t_p/\tau$. As such, while some, central, part of the input spectrum may experience a group delay, other parts of the spectrum will experience group advancement or neither delay nor advancement (see Figs. 6(b) and 6(c)).

It therefore follows that, regardless of the pulse length of the input Stokes pulse, the output pulse delays associated with SBS in the field of a CW monochromatic pump radiation cannot be attributed to SBS-induced group delay. They are predominantly a consequence of the phenomenon of SBS buildup.

## 5 Effect of pump spectral width on spectral broadening of SBS

It has been proposed in Ref. [19] that spectral broadening of the pump radiation may lead to comparable spectral broadening of the SBS gain bandwidth. This approach has

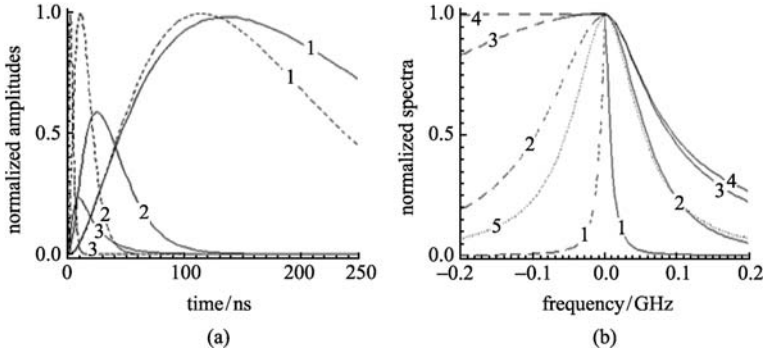


**Fig. 5** (a) Dynamics and (b) spectra of normalized acoustic wave amplitude (solid lines) for Stokes pulses of shape given by Eq. (11) (dashed lines) with $t_p = 200$ (1), 18 (2), 4 (3), and 0.5 (4) ns, $\tau = 18$ ns (Dotted line 5 in (b) is the Lorentzian-shaped spectrum with $\tau =$ 18 ns. Note that curves in (b) show half spectra of the pulses at LHS and of corresponding to them medium's response at RHS)

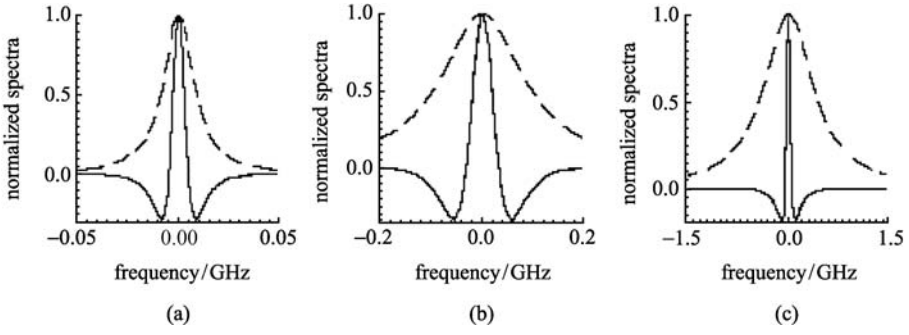


**Fig. 6** Relation between spectra of Stokes pulse and spectra of group index induced by this pulse. (a) $t_p$ = 200 ns; (b) $t_p$ = 18 ns; (c) $t_p$ = 4 ns

since been the focus of many publications [20–46]. In this section, we examine the validity of this assertion through an analytical solution of the SBS equations in the frequency domain. We show that the effect of spectral broadening of the pump radiation on the SBS bandwidth is in fact negligible.

To demonstrate this, we examine the spectral features of the medium's response and the Stokes emission through Fourier transformation of the Eqs. (4) and (5) using the following basic properties of Fourier transforms, $F(\omega) \equiv S[f(t)]$ [47],

$$\begin{aligned} S[f(t)] &= \int_{-\infty}^{\infty} f(t)\mathrm{e}^{-\mathrm{i}\omega t}\mathrm{d}t, \\ S\left[\frac{\mathrm{d}}{\mathrm{d}t}f(t)\right] &= \mathrm{i}\omega S[f(t)], \\ S[f_1(t)f_2(t)] &= \frac{1}{2\pi}\int_{-\infty}^{\infty} F_1(v)F_2(\omega - v)\mathrm{d}v, \end{aligned} \tag{14}$$

where $f(t)$ is a function of time. Here, $\omega$ and $v$ are Fourier transform frequencies, which are the difference frequencies of the acoustic, Stokes, and pump signals from their respective line centers. Equations (4) and (5) then give

$$\left(\frac{\Gamma_B}{2} - \mathrm{i}(\omega + \delta\Omega)\right)\tilde{\rho}^*(z,\omega) = \mathrm{i}\rho_0\frac{\partial\varepsilon}{\partial\rho}\frac{\Omega_B}{8\pi v_s^2}F_\rho(z,\omega) \tag{15}$$

and

$$\frac{\mathrm{d}\tilde{E}_S(z,\omega)}{\mathrm{d}z} + \mathrm{i}\omega\frac{n}{c}\tilde{E}_S(z,\omega) = -\mathrm{i}\frac{\omega_S}{2cn}\frac{\partial\varepsilon}{\partial\rho}F_E(z,\omega), \tag{16}$$

where

$$F_\rho(z,\omega) = \frac{1}{2\pi}\int_{-\infty}^{\infty}\tilde{E}_p'^{\,*}(v)\tilde{E}_S'(z,\omega - v)\mathrm{d}v, \tag{17}$$

$$F_E(z,\omega) = \frac{1}{2\pi}\int_{-\infty}^{\infty}\tilde{E}_p(v)\tilde{\rho}^*(z,\omega - v)\mathrm{d}v \tag{18}$$

are the functions that determine the spectrum of the driving force for the medium's response and generated Stokes field. Here, we have primed the Stokes and pump fields within Eq. (17), which are responsible for inducing the acoustic wave, to distinguish them from the generated Stokes field (LHS of Eq. (16)) and from the pump field, which generates the new Stokes field (the field $\tilde{E}_p(\omega)$ under the integral in Eq. (18)).

Note that in Eq. (15) $\delta\Omega$ is a detuning parameter, which can influence only the strength of the medium's response to the drive force at frequency, $\Omega$. (In the case of non-monochromatic pump and Stokes fields, $\delta\Omega$ can be considered as the difference between the central frequencies of their bandwidths.)

Consider the case of a typical SBS SL experiment in which the spectrum of the Stokes signal corresponds to that of a temporally smooth pulse and the spectrum of the pump radiation is the Fourier transform of a CW field, the amplitude of which is randomly fluctuating in time.

As seen, the RHSs of these equations are proportional to the convolution integrals of spectra $\tilde{E}_p'^{\,*}(\omega)$ and $\tilde{E}_S'(z,\omega)$ in Eq. (15) and $\tilde{E}_p(\omega)$ and $\tilde{\rho}^*(z,\omega)$ in Eq. (16), respectively.

Equation (15) is an algebraic equation, the solution of which gives the spectrum of the medium's response

$$\tilde{\rho}^*(z,\omega) = \mathrm{i}\rho_0\frac{\partial\varepsilon}{\partial\rho}\frac{\Omega_B}{8\pi v_s^2}\frac{F_\rho(z,\omega)}{(\Gamma_B/2) - \mathrm{i}(\omega + \delta\Omega)}. \tag{19}$$

The spectrum of the medium's response is then given by the modulus of $\tilde{\rho}^*(z,\omega)$, $|\tilde{\rho}(z,\omega)|$.

The spectrum of the Stokes field is described by the first-order differential equation (Eq. (16)), the solution of which is

$$\begin{aligned} &\left|\tilde{E}_S(z,\omega)\right| \\ &= \left|\mathrm{e}^{-\mathrm{i}\frac{\omega n}{c}z}\left[\tilde{E}_S(0,\omega) + \mathrm{i}\frac{\omega_S}{2nc}\frac{\partial\varepsilon}{\partial\rho}\int_0^z F_E(x,\omega)\mathrm{e}^{\mathrm{i}\frac{\omega n}{c}x}\mathrm{d}x\right]\right|, \end{aligned} \tag{20}$$

where $\tilde{E}_S(0,\omega)$ is the spectrum of an input Stokes signal at $z = 0$.

Equations (17)–(20) describe spectral features of the SBS-induced material response and Stokes field when both optical fields, pump and Stokes, are non-monochromatic. Note that solution Eq. (20) in the spectral domain is entirely consistent with the analytical solution of Eqs. (4) and (5), previously obtained in the temporal domain for stimulated scattering induced by non-monochromatic pump and monochromatic Stokes fields in Refs. [5,48–51] and for monochromatic pump and non-monochromatic Stokes fields in Ref. [52] (see Eq. (8)).

It is easily seen that the solution Eq. (20) for the Stokes field differs substantially from that usually deduced in textbooks from Eqs. (4) and (5) in the steady-state approximation (otherwise when both pump and Stokes fields are considered monochromatic),

$$E_{\mathrm{S}}(z) = E_{\mathrm{S}}(0)\mathrm{e}^{\frac{g_0|E_{\mathrm{p}}E_{\mathrm{p}}^*|z}{2(1-\mathrm{i}2\delta\Omega\Gamma_{\mathrm{B}}^{-1})}}, \tag{21}$$

which results from the equation for the Stokes field of the form [8,53]

$$\frac{\mathrm{d}E_{\mathrm{S}}(z)}{\mathrm{d}z} = \left[\frac{g_0|E_{\mathrm{p}}E_{\mathrm{p}}^*|}{2(1-\mathrm{i}2\delta\Omega\Gamma_{\mathrm{B}}^{-1})}\right]E_{\mathrm{S}}(z). \tag{22}$$

Here, it is again important to remember that $\delta\Omega$ is a detuning parameter, the value of which ($\delta\Omega = \Omega - \Omega_{\mathrm{B}}$) is the difference between the frequencies of the monochromatic pump and Stokes fields as chosen ($\Omega = \omega_{\mathrm{p}} - \omega_{\mathrm{S}}$) and the resonant Brillouin frequency, $\Omega_{\mathrm{B}}$, and $g_0$ is the standard steady-state SBS gain coefficient. Equation (22) means that the Stokes field is amplified in the medium with a gain proportional the pump radiation intensity. To appreciate the difference between this case and our case, let us consider both pump and Stokes fields in Eqs. (15)–(20) to be monochromatic. The spectra of the amplitudes of driving forces and the spectra of the medium's response then reduce to δ-functions at $\omega = 0$ and these depend on $z$ only. The equation for the Stokes field is then

$$\frac{\mathrm{d}E_{\mathrm{S}}(z)}{\mathrm{d}z} = \left[\frac{g_0(E_{\mathrm{p}}'^{\,*}E_{\mathrm{S}}'(z))}{2(1-\mathrm{i}2\delta\Omega\Gamma_{\mathrm{B}}^{-1})}\right]E_{\mathrm{p}}. \tag{23}$$

The physical meaning of Eq. (23) is substantially different from that of Eq. (22), although their mathematical forms may look similar. Equation (23) describes the spatial evolution of the amplitude of the Stokes field, which results from reflection of the pump field by the induced acoustic wave. Since the Stokes field on the RHS of Eq. (23) is responsible for creating the acoustic wave, it is not the same as the reflected Stokes field on the LHS of this equation; therefore, it is distinguished by its prime. Although, for this monochromatic case, the Stokes fields have the same frequency, their roles still remain physically distinct as in our general treatment above. Such distinction is not made in the textbook treatment that leads to Eq. (22) and to its familiar exponential solution Eq. (21), which displays "gain" and a "modified propagation constant" for the Stokes field (see Ref. [10]). Evidently, the solution for Eq. (23) cannot be the same. As such, although the RHS of this equation has both real and imaginary parts (in the case of non-zero detuning, $\delta\Omega$), this does not modify the propagation constant for the reflected Stokes field; therefore, it can have no bearing on changing the refractive and group indices for this field.

Returning now to the solutions Eqs. (17)–(20) of equations Eqs. (15) and (16) for the general case in which either one of the fields or both have non-zero bandwidth, they display three important features of the SBS interaction: 1) the external input Stokes signal, as seen in Eq. (20), propagates through a non-absorbing medium without gain or measurable loss (its energy losses for creating the acoustic wave is usually negligible), consistent with earlier analysis in the temporal domain (see Eq. (8)); 2) the SBS-generated Stokes signal is a result of reflection of the pump radiation by the acoustic wave, which is created by the pump and the original Stokes fields (see Eqs. (4) and (15)); and 3) each spectral component of the generated Stokes signal arises from a range of spectral components of the non-monochromatic pump and Stokes fields (see Eqs. (18) and (20)).

To see the consequences of this, consider the case when the growth of the Stokes field along $z$ is small. As such, the $z$ dependence of $\tilde{E}_{\mathrm{S}}(z,\omega)$ and $\tilde{\rho}^*(z,\omega)$ is dropped. While this approximation does not account for gain narrowing of the SBS spectrum, typical for higher amplification [8,48], it still captures reasonably well the trends in the spectral features of the Stokes field, $\tilde{E}_{\mathrm{S}}(z,\omega)$, the medium response, $|\tilde{\rho}(\omega)|$, and the SBS gain and the modified refractive and group indices.

It follows from Eq. (20) that the output spectrum of the Stokes signal, $|\tilde{E}_{\mathrm{S}}(\omega)|$, is the sum of the Fourier spectra of the input Stokes signal, $|\tilde{E}_{\mathrm{S}}(0,\omega)|$, and the convoluted spectrum of the pump field and medium's excitation, characteristics that are described by the function $F_{\mathrm{E}}(\omega)$ (see Eq. (18)). The latter is the SBS-induced contribution to the Stokes signal and is determined by which of $\tilde{E}_{\mathrm{p}}(\omega)$ or $\tilde{\rho}^*(\omega)$ is spectrally broadest. These spectral features of the output Stokes radiation are consistent with those predicted earlier in the low gain approximation using the temporal domain treatment of stimulated Raman scattering [48,49] and SBS [8] with non-monochromatic pump fields.

In contrast to the spectral features of the Stokes emission, those of the medium's response, $|\tilde{\rho}(\omega)|$, have, to date, received little attention. According to Eq. (19), this case is not as straightforward as that of the Stokes spectrum since a Lorentzian-shaped multiplier of bandwidth $\Gamma_{\mathrm{B}}$ appears in addition to the convolution integral, $F_{\rho}(\omega)$. From Eq. (19), $|\tilde{\rho}(\omega)|$ is given as

$$|\tilde{\rho}(\omega)| = \rho_0 \frac{\partial \varepsilon}{\partial \rho} \frac{\Omega_B}{8\pi v_s^2} \frac{|F_\rho(\omega)|}{\sqrt{\Gamma_B^2/4 + (\omega + \delta\Omega)^2}}. \quad (24)$$

Examples of the spectra, $|\tilde{\rho}(\omega)|$, are shown in Fig. 7 by solid curves for $\delta\Omega = 0$ (Fig. 7(a)) and $\delta\Omega = 0.1$ GHz (Fig. 7(b)).

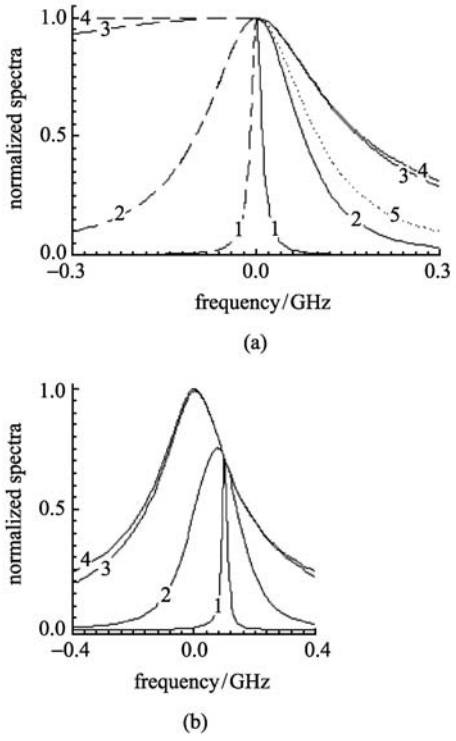


**Fig. 7** (a) LHS and RHS halves of (symmetrical) spectra of $|F_\rho(\omega)|$ (dashed lines) and spectra of $|\tilde{\rho}(\omega)|$ (solid lines), respectively, for spectral widths of $F_\rho(\omega)$ 0.02 (1), 0.2 (2), 2 (3), and 20 (4) GHz, when $\Gamma_0 = 0.2$ GHz and $\delta\Omega = 0$ (the dotted line 5 is the Lorentzian-shaped spectrum with $\Gamma_0 = 0.2$ GHz); (b) spectra of $|\tilde{\rho}(\omega)|$ for the same spectral widths of $F_\rho(\omega)$ when $\delta\Omega = 0.1$ GHz

It follows from Eq. (24) that, when the spectral width of the driving force, $|F_\rho(\omega)|$ (shown by dashed curves in Fig. 7(a)), is narrower than $\Gamma_B$, the width, $\Gamma$, and center frequency of the medium's spectrum, $|\tilde{\rho}(\omega)|$, is determined by $|F_\rho(\omega)|$ (the convolution of $\tilde{E}_p^*(\omega)$ and $\tilde{E}_S(\omega)$ as given in Eq. (17)), the central frequency of which is detuned by $\delta\Omega$ as shown by curve 1 in Fig. 7(b). Non-zero detuning $\delta\Omega$ results also in decreased amplitude of the medium's response (compare solid curves 1 of Figs. 7(a) and 7(b)). As the spectral width of $|F_\rho(\omega)|$ increases, $\Gamma$ grows, and for $|F_\rho(\omega)| > \Gamma_B$, it saturates at ~$1.7\Gamma_B$ (solid curves 3 and 4 in Fig. 7(a)), and the effect of the detuning $\delta\Omega$ on the features of the medium's spectrum becomes negligible (compare solid curves 3 and 4 in Figs. 7(a) and 7(b)). In essence, this means that, irrespective of how broad the bandwidth of the broadband pump and/or Stokes emission is, the bandwidth of the material response spectrum is predominantly determined by the features of the material and can never be much greater than that of the medium's resonant response (~$\Gamma_B$). This is exactly the features expected from an externally driven damped resonant oscillator (see Eq. (2)).

## 6 Conclusion

We have shown through analytical analysis of the basic SBS equations that SBS amplification of an external Stokes pulse cannot give rise to group index-induced delay of this pulse. The output Stokes pulse delays widely reported in the literature can be accounted for by the time taken for SBS to be established in the medium, the so-called inertial buildup time of SBS. It is also shown that spectral broadening of the pump radiation by any reasonable amount has next to no effect on the SBS spectral bandwidth of the excited acoustic wave in the medium, which is commonly believed to determine the SBS gain bandwidth [6–8].

**Acknowledgements** The authors wish to thank Profs. I. G. Zubarev and J. K. Knight for fruitful discussion. This work was supported by the Engineering and Physical Sciences Research Council (UK) (No. EP/E029493/1), the Scottish University Physics Alliance, and the Educational Scientific Complex of the Lebedev Physical Institute of the Russian Academy of Sciences.

## References

1. Brillouin L. Wave Propagation and Group Velocity. New York: Academic Press, 1960
2. Boyd R W, Gauthier D J. "Slow" and "fast" light. Progress in Optics, 2002, 43(6): 497–530
3. Gauthier D J. Slow light brings faster communications. Physics World, 2005, 18: 30–32
4. Thevenaz L. Slow and fast light in optical fibres. Nature Photonics, 2008, 2(8): 474–481
5. Kroll N M. Excitation of hypersonic vibrations by means of photoelastic coupling of high-intensity light waves to elastic waves. Journal of Applied Physics, 1965, 36(1): 34–43
6. Zeldovich B Ya. Time of establishment of stationary regime of stimulated light scattering. Journal of Experimental and Theoretical Physics Letters, 1972, 15: 158–159
7. Okawachi Y, Bigelow M S, Sharping J E, Zhu Z, Schweinsberg A, Gauthier D J, Boyd R W, Gaeta A L. Tunable all-optical delays via Brillouin slow light in an optical fiber. Physical Review Letters, 2005, 94(15): 153902
8. Zeldovich B Ya, Pilipetskii N F, Shkunov V V. Principles of Phase Conjugation. Berlin: Springer Verlag, 1985
9. Song K Y, Herraez M G, Thevenaz L. Observation of pulse delaying and advancement in optical fibers using stimulated Brillouin scattering. Optics Express, 2005, 13(1): 82–88
10. Zhu Z, Gauthier D J, Okawachi Y, Sharping J E, Gaeta A L, Boyd R W, Willner A E. Numerical study of all-optical slow-light delays via stimulated Brillouin scattering in an optical fiber. Journal of the

Optical Society of American B, 2005, 22(11): 2378–2384
11. Bronshtein I N, Semendyaev K A. A Guide-Book to Mathematics. Zurich: Verlag Harri Deutsch, 1973
12. Pohl D, Kaiser W. Time-resolved investigations of stimulated Brillouin scattering in transparent and absorbing media: determination of phonon lifetimes. Physical Review B, 1970, 1(1): 31–43
13. Kovalev V I, Harrison R G. Threshold for stimulated Brillouin scattering in optical fiber. Optics Express, 2007, 15(26): 17625–17630
14. Pinnow D A. Guide lines for the selection of acoustooptic materials. IEEE Journal of Quantum Electronics, 1970, 6(4): 223–238
15. Agrawal G P. Nonlinear Fiber Optics. 2nd ed. Boston: Academic, 1995
16. Kovalev V I, Harrison R G. Observation of inhomogeneous spectral broadening of stimulated Brillouin scattering in an optical fiber. Physical Review Letters, 2000, 85(9): 1879–1882
17. Kovalev V I, Harrison R G. Waveguide-induced inhomogeneous spectral broadening of stimulated Brillouin scattering in optical fiber. Optics Letters, 2002, 27(22): 2022–2024
18. Kalosha V P, Cheng L, Bao X. Slow and fast light via SBS in optical fibers for short pulses and broadband pump. Optics Express, 2006, 14(26): 12693–12703
19. Stenner M D, Neifeld M A, Zhu Z, Dawes A M C, Gauthier D J. Distortion management in slow-light pulse delay. Optics Express, 2005, 13(25): 9995–10002
20. Herraez M G, Song K Y, Thevenaz L. Arbitrary-bandwidth Brillouin slow light in optical fibers. Optics Express, 2006, 14(4): 1395–1400
21. Minardo A, Bernini R, Zeni L. Low distortion Brillouin slow light in optical fibers using AM modulation. Optics Express, 2006, 14(13): 5866–5876
22. Shumakher E, Orbach N, Nevet A, Dahan D, Eisenstein G. On the balance between delay, bandwidth and signal distortion in slow light systems based on stimulated Brillouin scattering in optical fibers. Optics Express, 2006, 14(13): 5877–5884
23. Zhu Z, Gauthier D J. Nearly transparent SBS slow light in an optical fiber. Optics Express, 2006, 14(16): 7238–7245
24. Schneider T, Junker M, Lauterbach K U, Henker R. Distortion reduction in cascaded slow light delays. Electronics Letters, 2006, 42(19): 1110–1112
25. Zadok A, Eyal A, Tur M. Extended delay of broadband signals in stimulated Brillouin scattering slow light using synthesized pump chirp. Optics Express, 2006, 14(19): 8498–8505
26. Chin S, Gonzalez-Herraez M, Thevenaz L. Zero-gain slow and fast light propagation in an optical fiber. Optics Express, 2006, 14(22): 10684–10692
27. Schneider T, Junker M, Lauterbach K U. Potential ultra wide slow-light bandwidth enhancement. Optics Express, 2006, 14(23): 11082–11087
28. Kalosha V P, Cheng L, Bao X. Slow and fast light via SBS in optical fibers for short pulses and broadband pump. Optics Express, 2006, 14(26): 12693–12703
29. Zhu Z, Dawes A M C, Gauthier D J, Zhang L, Willner A E. Broadband SBS slow light in an optical fiber. Journal of Lightwave Technology, 2007, 25(1): 201–206
30. Song K Y, Hotate K. 25 GHz bandwidth Brillouin slow light in optical fibers. Optics Letters, 2007, 32(3): 217–219
31. Lu Z, Dong Y, Li Q. Slow light in multi-line Brillouin gain spectrum. Optics Express, 2007, 15(4): 1871–1877
32. Zhang B, Yan L, Fazal I, Zhang L, Willner A E, Zhu Z, Gauthier D J. Slow light on Gbit/s differential-phase-shift-keying signals. Optics Express, 2007, 15(4): 1878–1883
33. Yi L, Zhan L, Hu W, Xia Y. Delay of broadband signals using slow light in stimulated Brillouin scattering with phase-modulated pump. IEEE Photonics Technology Letters, 2007, 19(8): 619–621
34. Zhang B, Zhang L, Yan L S, Fazal I, Yang J Y, Willner A E. Continuously-tunable, bit-rate variable OTDM using broadband SBS slow-light delay line. Optics Express, 2007, 15(13): 8317–8322
35. Shi Z, Pant R, Zhu Z, Stenner M D, Neifeld M A, Gauthier D J, Boyd R W. Design of a tunable time-delay element using multiple gain lines for increased fractional delay with high data fidelity. Optics Letters, 2007, 32(14): 1986–1988
36. Schneider T, Henker R, Lauterbach K U, Junker M. Comparison of delay enhancement mechanisms for SBS-based slow light systems. Optics Express, 2007, 15(15): 9606–9613
37. Yi L, Jaouen Y, Hu W, Zhou J, Su Y, Pincemin E. Simultaneous demodulation and slow light of differential phase-shift keying signals using stimulated-Brillouin-scattering-based optical filtering in fiber. Optics Letters, 2007, 32(21): 3182–3184
38. Yi L, Jaouen Y, Hu W, Su Y, Bigo S. Improved slow-light performance of 10 Gb/s NRZ, PSBT and DPSK signals in fiber broadband SBS. Optics Express, 2007, 15(25): 16972–16979
39. Song K Y, Abedin K S, Hotate K. Gain assisted superluminal propagation in tellurite glass fiber based on stimulated Brillouin scattering. Optics Express, 2008, 16(1): 225–230
40. Pant R, Stenner M D, Neifeld M A, Gauthier D J. Optimal pump profile designs for broadband SBS-based slow light systems. Optics Express, 2008, 16(4): 2764–2777
41. Ren L, Tomita Y. Reducing group-velocity-dispersion-dependent broadening of stimulated Brillouin scattering slow light in an optical fiber by use of a single pump laser. Journal of the Optical Society of American B, 2008, 25(5): 741–746
42. Sakamoto T, Yamamoto T, Shiraki K, Kurashima T. Low distortion slow light in flat Brillouin gain spectrum by using optical frequency comb. Optics Express, 2008, 16(11): 8026–8032
43. Wang S, Ren L, Liu Y, Tomita Y. Zero-broadening SBS slow light propagation in an optical fiber using two broadband pump beams. Optics Express, 2008, 16(11): 8067–8076
44. Schneider T, Henker R, Lauterbach K U, Junker M. Distortion reduction in slow light systems based on stimulated Brillouin scattering. Optics Express, 2008, 16(11): 8280–8285
45. Schneider T. Time delay limits of stimulated-Brillouin-scattering-based slow light systems. Optics Letters, 2008, 33(13): 1398–1400
46. Cheng A, Fok M P, Shu C. Wavelength-transparent, stimulated-Brillouin-scattering slow light using cross-gain-modulation-based wavelength converter and Brillouin fiber laser. Optics Letters, 2008, 33(22): 2596–2598
47. Korn G A, Korn T M. Manual of Mathematics. New York: McGraw-Hill, 1967
48. Akhmanov S A, Dyakov Y E, Chirkin A S. Introduction to Statistical Radiophysics and Optics. Berlin: Springer, 1988

49. Carman R L, Shimizu F, Wang C S, Bloembergen N. Theory of Stokes pulse shapes in transient simulated Raman scattering. Physical Review A, 1970, 2(1): 60–72
50. Akhmanov S A, Drabovich K N, Sukhorukov A P, Chirkin A S. Stimulated Raman scattering in a field of ultrashort light pulses. Soviet Journal of Experimental and Theoretical Physics, 1971, 32: 266–273
51. Bel'dyugin I M, Efimkov V F, Mikhailov S I, Zubarev I G. Amplification of weak Stokes signals in the transient regime of stimulated Brillouin scattering. Journal of Russian Laser Research, 2005, 26(1): 1–12
52. Kovalev V I, Kotova N E, Harrison R G. Effect of acoustic wave inertia and its implication to slow light via stimulated Brillouin scattering in an extended medium. Optics Express, 2009, 17(4): 2826–2833
53. Milonni P W, Eberly J H. Lasers. New York: Wiley, 1988